



Bio-adsorption properties of Rhodamine B from aqueous solution onto natural camphor tree leaf powder

Huihui Gan, Huining Zhang*, Jiawei Cai, Huixia Jin, Kefeng Zhang

School of Civil Engineering and Architecture, Ningbo Institute of Technology, Zhejiang University, 1 South Qianhu Road, Ningbo 315100, P.R. China, email: huihuiGAN1987@126.com (H. Gan), Tel./Fax: +86 574 88130283; emails: zhanghnnit@163.com (H. Zhang), 1390439390@qq.com (J. Cai), hxjin@nit.net.cn (H. Jin), kfzhang@nit.net.cn (K. Zhang)

Received 22 April 2015; Accepted 30 June 2015

ABSTRACT

The potential of camphor tree leaf powder (CALP) to remove Rhodamine B (RhB) from aqueous solution was evaluated. The CALP was characterized by the scanning electron microscope and Fourier transform infrared technique, respectively. The effects of contact time, initial RhB concentrations, solution pH, and strength of the coexisting cations and anions upon the RhB adsorption were evaluated. The CALP had buffering action on the RhB/CALP system to maintain the solution pH in the range of 7. The Langmuir, Freundlich, and Koble–Corrigan isotherm models were used to analyze the adsorption behavior and the Koble–Corrigan isotherm fits the equilibrium data best ($R^2 > 0.99$). The kinetic studies indicated that the adsorption process was fitted well with the pseudo-second-order model with rate constants (k_2) in the range of 0.2586–3.0489 g/mg/min, suggesting that the adsorption might be a chemisorption process. The thermodynamic parameters indicated that adsorption process was feasible and spontaneous.

Keywords: Adsorption; Camphor tree leaf powder; Rhodamine B; Isotherm; Kinetics

1. Introduction

Dyestuffs are one of the typical contaminants in aquatic environments. Over 7×10^5 tons of dyes are annually produced in the world, and more than 15% of which are released into the environment during manufacturing, processing, and using [1–3]. Synthetic dyes are known to cause visible pollution in effluent water and may retard photosynthesis and biota growth. Rhodamine B (RhB) is a xanthene synthetic dye and its carcinogenicity, reproductive and developmental toxicity, neurotoxicity, and chronic toxicity have been experimentally proven [4,5]. To avoid the

environmental contamination engendered from dye-stuffs, efficient and low-cost methods have to be developed.

Dyes usually have good physicochemical, thermal, and optical stability due to the complex aromatic molecules, and are generally resistant to biodegradation. Various physicochemical techniques, such as adsorption, chemical oxidation, electrocoagulation, and advance oxidation processes, have been applied for the removal of dyes from wastewater. Adsorption has been found to be one of the most efficient physicochemical processes, for the removal of dyes from aqueous effluents in terms of simplicity of the operation and nearly no harmful by-products [6,7]. While activated carbon is the widely used adsorbent, carbon

*Corresponding author.

adsorption remains a costly treatment process. Until now, several low-cost adsorbents have been reported for dye removal such as fly ash [8], kaolinite [9], and magnesium aluminate [10]. Natural solid material can be considered more attractive also, besides being aligned with the concepts of green chemistry. Natural products, usually considered waste, such as wheat straw [11], bamboo [12], chir pine sawdust [13], broad bean peels [14], pine cone [15], and water chestnut peel [16], have been employed to remove the color dyes from water. Natural products, such as tree leaves, usually contain components, such as, polyphenolics, plant pigments, and protein, which can provide active sites for dye binding [17].

In the present work, the natural camphor tree leaf powder (CALP) was used as a low-cost adsorbent for the removal of RhB from aqueous solution. The effects of contact time and initial RhB concentration, pH of the RhB solution, temperature, and strength of the coexisting cations and anions on the adsorption were investigated. The adsorption kinetics and isotherms for RhB onto the CALP were also discussed.

2. Methods

2.1. Preparation of adsorbent and adsorbate

Camphor tree leaves were collected from the Ningbo, China. The leaves were washed with distilled water to remove dusts and water soluble impurities on the surface. Leaves were firstly dried at room temperature and then dried at 110°C for 12 h in an air oven. The dried leaves are ground by grinder and sieved to obtain particle size lower than 0.15 mm (100 mesh) diameter. The prepared CALPs were kept in desiccators for use in adsorption studies.

RhB was purchased from Sinopharm Chemical Reagent Co. Ltd, China. The stock solution of RhB was prepared by dissolving a required amount of RhB in deionized water.

2.2. Characterizations

The chemical bonds of CALPs were detected by Fourier transform infrared (FT-IR) spectroscopy (Nexus, Thermo Nicolet). The morphologies of the powders were analyzed by a FEI Quanta 200 scanning electron microscope (SEM) with an acceleration voltage of 25 kV.

2.3. Adsorption experiments

All adsorption experiments were carried out on a thermostated shaker (KYC-1102C, China) operated at

170 rpm. Deionized water was used throughout the experiment. The concentration of RhB aqueous solution was analyzed using a UV-vis spectrophotometer (UV2800, China) at its maximum absorption wavelength of 554 nm. The effect of the initial pH on the amount of adsorbed RhB was studied over a pH range of 2–12. The pH of RhB solutions was adjusted by the addition of HCl or NaOH solution (0.1 mol/L). To investigate the effect of coexisting ions, the concentrations of ions in solution were set as 0.02, 0.05, 0.10, 0.15, and 0.2 mol/L. The cations were prepared by dissolving KCl, NaCl, CaCl₂·2H₂O, and MgCl₂·6H₂O, respectively. The anions were prepared by dissolving NaCl, Na₂SO₄, Na₂CO₃, and NaNO₃, respectively. Equilibrium behaviors of RhB on the CALP were studied at three temperatures (30, 40, and 50°C). Adsorption kinetic experiments were done by keeping 0.6 g of adsorbent and 200 mL of MB aqueous solution of varying concentration in a series of 250 mL flasks, maintained at constant temperature.

3. Results and discussion

3.1. Characterization of the adsorbent

The infrared spectra of the CALP before and after RhB adsorption is shown in Fig. 1. The broadband at 3418 cm⁻¹ was due to the O–H stretching vibration of alcohols, phenols, and carboxylic acids, thus showing the presence of “free” hydroxyl groups on the CALP surface [18]. The broad absorption peaks at 2,918 and 2,850 cm⁻¹ were assigned to the stretching vibration of C–H bond. The peak at 1,613 cm⁻¹ was a characteristic of the carbonyl group stretching. The adsorption peaks observed around 1,063 cm⁻¹ could be attributed to the

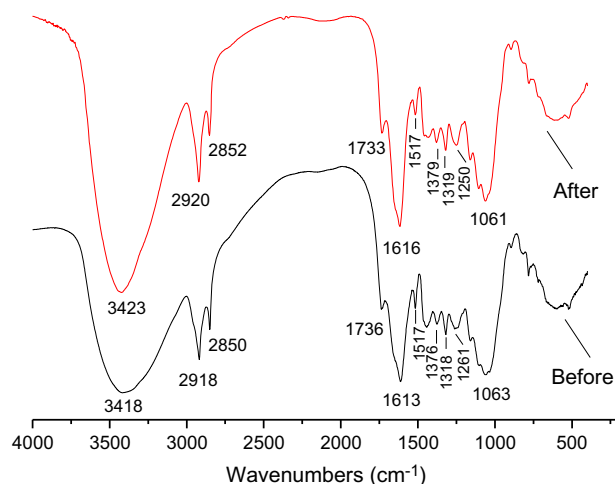


Fig. 1. FT-IR spectra of CALP.

stretch vibration of C–O–C of cellulose present in the material. As observed, the wave numbers in the FT-IR spectrum of CALP after adsorption of RhB were shifted from 3,318, 2,918, 1,613, and 1,063 cm^{-1} to 3,423, 2,920, 1,616, and 1,061 cm^{-1} , respectively. The changes observed suggested that the interactions of dye molecules with the functional groups of CALP in the adsorption process and the hydroxyl and carboxyl groups might be the active groups for RhB adsorption. SEM micrographs of the CALP are shown in Fig. 2. It can be seen that the CALP exhibited irregular morphology and coarse porous surface. On the basis of this fact, it can be concluded that the CALP adsorbent presents an adequate morphology adsorption.

3.2. Effect of pH value on adsorption

The effect of the pH of the original solution on the adsorption capacity of RhB is shown in Fig. 3. It can be seen that the amount adsorbed decreased from 6.5 to 6.07 mg/g for CALP and the removal of RhB decreased 6.4% with an increase in the solution pH from 2.09 to 4.13. It is observed that the CALP adsorbs RhB favorably at lower pH. It is interesting that the amount adsorbed for RhB remained approximately constant in the pH range from 4.13 to 9.92 and decreased slightly as the pH increased from 9.92 to 10.97. The changes in solution pH with different times for adsorption of RhB by CALP are shown in Fig. 4. In Fig. 4, it is found that the RhB solution pH changes significantly after adding the adsorbent CALP and the changing trend is almost the same, which is close to neutral. This observation is important that the CALP

has buffering action on the RhB/CALP system to maintain the pH in the range of 7. The result could be attributed that the hydroxyl groups on surface of the CALP have amphoteric behavior and simultaneously exhibit buffering in acidic solution and basic solution.

3.3. Effect of initial dye concentration and time

Fig. 5 shows the effect of initial dye concentration and contact time on adsorption capacity of the CALP. It can be seen that the initial adsorption was rapid in the first 2 min and thereafter adsorption was gradual and equilibrium was reached within 100 min. The adsorption amount of RhB onto the CALP increased from 3.0 to 52 mg/g with an increase in the initial RhB concentration from 10 to 200 mg/L. It is clear that the adsorption process is highly dependent on initial concentration of solution. The driving force of the concentration gradient is enhanced, as the initial RhB concentration is increased.

3.4. Effect of the coexisting cations and anions

It was important to discuss the effect of coexisting cations for adsorption of RhB onto the CALP because dyeing wastewater usually contains high salt concentration. As shown in Fig. 6, K^+ , Na^+ , Ca^{2+} , and Mg^{2+} had little significant effect on RhB adsorption. The fact that these cations had little effect on adsorption of RhB, was an advantage for the CALP to be used as adsorbent to remove the dye pollutants from wastewater. The effect of coexisting anions for adsorption of

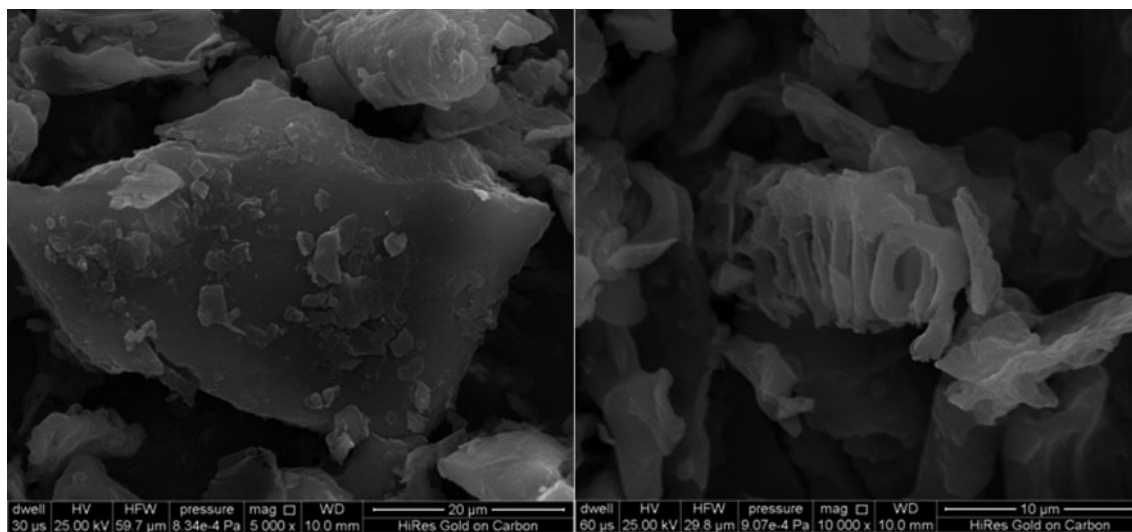


Fig. 2. SEM images of CALP.

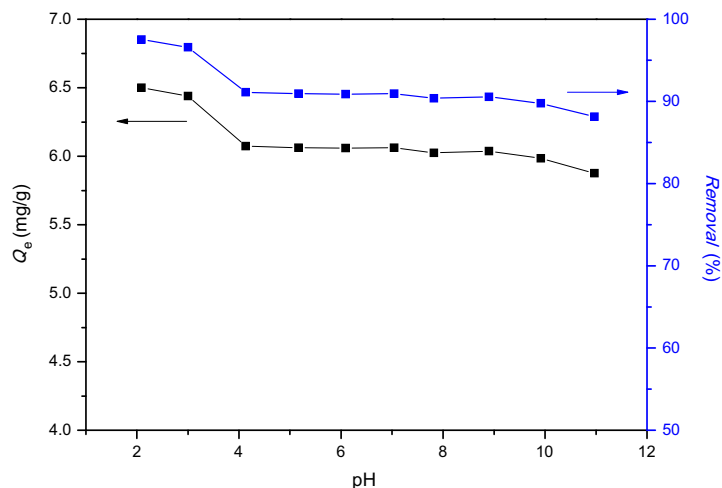


Fig. 3. Effect of initial pH on adsorption of RhB by CALP (temperature = 30°C, $t = 150$ min, $C_0 = 20$ mg/L, dosage = 3 g/L).

RhB onto the CALP was also analyzed. It can be seen from Fig. 7 that, the Cl^- , NO_3^- , and SO_4^{2-} had little significant effect on ammonium adsorption. CO_3^{2-} greatly reduces the adsorption of RhB because the hydrolyzation increases the solution pH. The amount adsorbed for the CALP decreased with an increase in the solution pH, which is conformed in Fig. 4.

3.5. Adsorption kinetics

To analyze the kinetic mechanism of RhB onto the CALP, the pseudo-first-order and pseudo-second-order,

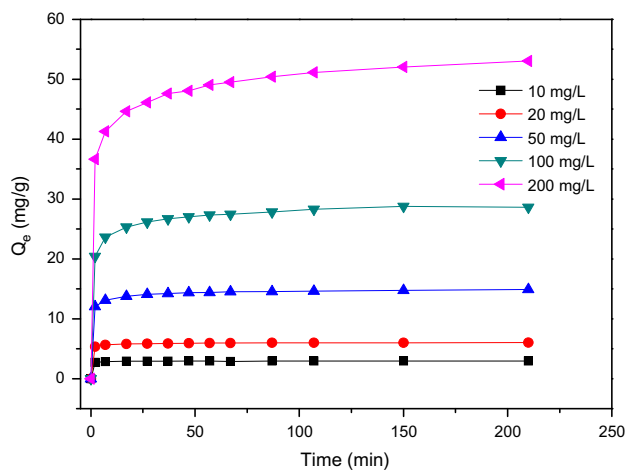


Fig. 5. Effect of contact time on adsorption capacity (temperature = 30°C, dosage = 3 g/L).

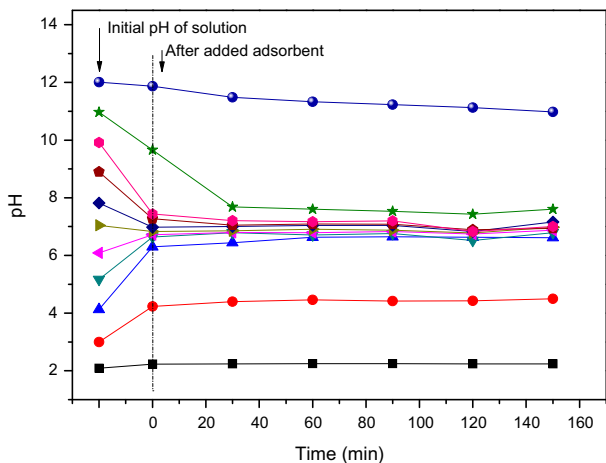


Fig. 4. Change of pH on adsorption of RhB by CALP (temperature = 30°C, $t = 150$ min, $C_0 = 20$ mg/L, dosage = 3 g/L).

film-diffusion models, and intraparticle-diffusion models were used [19].

The pseudo-first-order equation can be expressed as:

$$\log(q_e - q_t) = \log q_e - \frac{k_1 t}{2.303} \tag{1}$$

where q_e and q_t are the amounts of RhB adsorbed at equilibrium and at contract time t (mg/g), respectively, and k_1 is the pseudo-first-order rate constant (min^{-1}). The values of k_1 and q_e were determined from the intercept and the slope of the plot of $\log(q_e - q_t)$ vs. t .

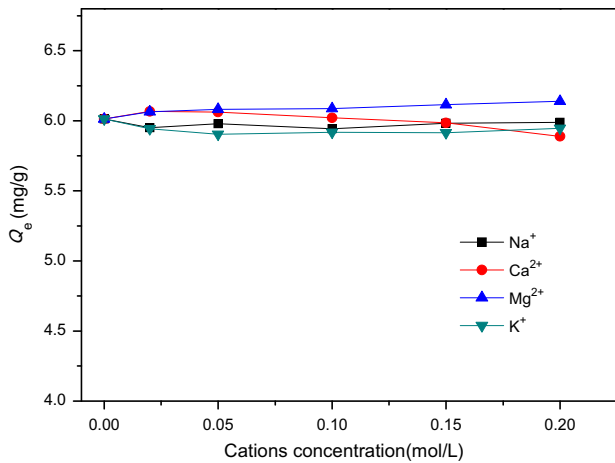


Fig. 6. Effect of coexisting cations on the adsorption of RhB (temperature = 30°C, C₀ = 20 mg/L, dosage = 3 g/L).

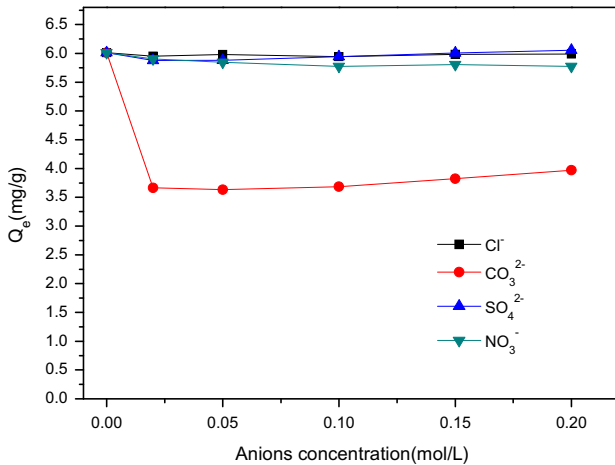


Fig. 7. Effect of coexisting anions on the adsorption of RhB (temperature = 30°C, C₀ = 20 mg/L, dosage = 3 g/L).

Pseudo-second-order rate equation can be expressed in the following form:

$$\frac{t}{q_t} = \frac{1}{k_2 q_e^2} + \frac{t}{q_e} \quad (2)$$

where k_2 is the pseudo-second-order rate constant [g/(mg min)]. The values of k_2 and q_e were determined from the intercept and slope of the plot of t/q_t vs. t .

The sorption rate constant and correlation coefficients for the pseudo-first-order and pseudo-second-order models are shown in Table 1. The values of R^2 (0.9993–0.9999) obtained from pseudo-second-order

model were larger than those of the pseudo-first-order model, which indicate that the adsorption data conform well to the pseudo-second-order kinetics for the entire adsorption process. The linear plot of t/Q_t vs. t for the pseudo-second-order kinetic model is shown in Fig. 8. The result suggests that the pseudo-second order kinetic model, based on the assumption that the rate-controlling step may be chemical sorption involving valence forces through sharing or exchanging electrons between adsorbent and adsorbate, provides the best correlation of the data [20,21].

Liquid-film diffusion can be explained by the following equation:

$$-\ln\left(1 - \frac{q_t}{q_e}\right) = k_{fd}t \quad (3)$$

The film-diffusion plots (Fig. 9) were found to be linear ($R^2 = 0.9095$ – 0.9767), thereby confirming the applicability of the model. The plots did not pass through the origin indicating that the liquid-film diffusion was not the predominant mechanism for RhB adsorption onto the CALP. The values of k_{fd} and R^2 obtained were listed in Table 2. The adsorption rate constant, k_{fd} , was in 0.02352–0.04123 1/min range.

To determine the diffusion mechanism of adsorption process, the intraparticle diffusion equation [22–24] is given by:

$$q_t = k_3 t^{1/2} + C \quad (4)$$

where k_3 is the rate constant of intraparticle diffusion (mg/g min^{1/2}), which is determined from the linear plot of q_t vs. $t^{1/2}$, and it is usually used to compare the mass transfer rates. The value of C relates to the thickness of boundary layer. As shown in Fig. 10, the plot of q_t against $t^{1/2}$ for different initial concentrations presented multilinearity relation, indicating that two or more steps take place. The first step is the instantaneous external surface adsorption. The second step is the gradual adsorption stage, where intraparticle diffusion is rate controlling. The third stage refers to the final equilibrium stage where intraparticle diffusion starts to slow down due to extremely low-adsorbate concentrations in the solution [25]. As seen from Fig. 10, none of the lines passed through the origin indicates that the intraparticle diffusion was not only rate-controlling step [26,27]. The values of k_t and C obtained from the second stage linear regression analysis are listed in Table 2. It is seen that the C values increased with an increase in the initial adsorbate concentration, which reflected the increase in thickness of

Table 1

Pseudo-first-order and pseudo-second-order kinetic parameters for the adsorption of RhB onto the CALP

C_0 (mg/L)	$q_{e(\text{exp})}$ (mg/g)	Pseudo-first-order kinetic model			Pseudo-second-order kinetic model			
		k_1 (min^{-1})	$q_{e(\text{cal})}$ (mg/g)	R^2	k_2 (g/mg min)	$q_{e(\text{cal})}$ (mg/g)	h_0 (mg/g/min)	R^2
10	2.9539	0.03974	0.1548	0.8766	3.0489	2.9500	8.9944	0.9999
20	5.9972	0.04123	0.5243	0.9767	1.4685	6.0274	8.8511	0.9999
50	14.7548	0.02938	1.9059	0.9247	0.6278	14.9276	9.3721	0.9999
100	28.7639	0.02352	5.9093	0.9095	0.3901	28.9519	11.2931	0.9997
200	52.0509	0.02459	12.6887	0.9679	0.2586	53.4188	13.8141	0.9993

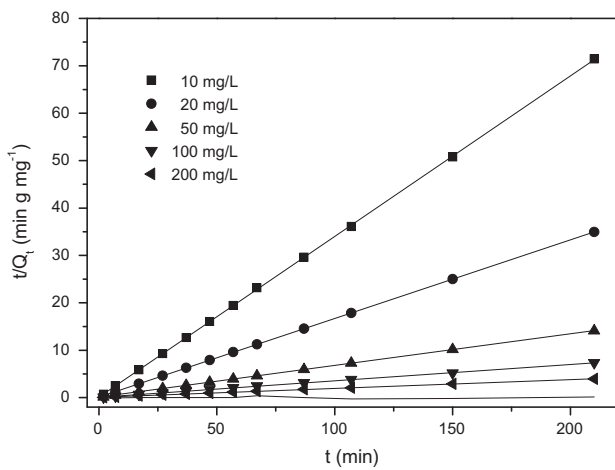


Fig. 8. The pseudo-second-order models for the adsorption of RhB onto the CALP.

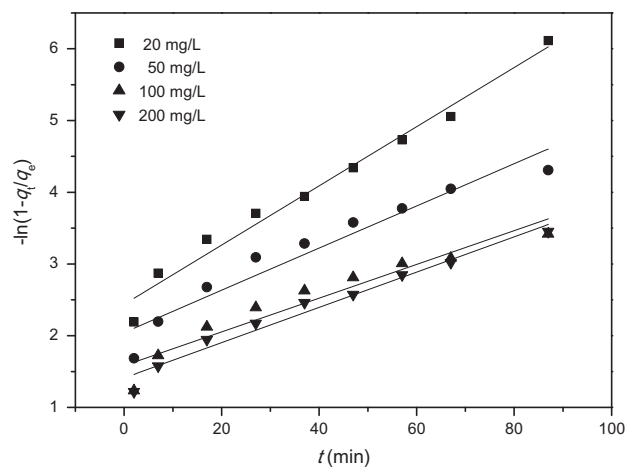


Fig. 9. The liquid-film diffusion plots for the adsorption of RhB onto the CALP.

the boundary layer and lead to the greater contribution of surface sorption in the rate-controlling step.

3.6. Adsorption isotherms

The adsorption isotherms play an important role in understanding the mechanism of adsorption. The surface phase may be considered as a monolayer or

multilayer. Several isotherm models related to adsorption equilibrium, in order to describe the interactions between the adsorbate and adsorbent, are presented in the literature [28]. The Langmuir adsorption isotherm is given as:

$$\frac{C_e}{q_e} = \frac{C_e}{q_m} + \frac{1}{q_m k_b} \tag{5}$$

Table 2

The liquid-film diffusion and intraparticle-diffusion model parameters for the adsorption of RhB onto the CALP

Kinetic model	Kinetic parameters	C_0 (mg/L)			
		20	50	100	200
Liquid-film diffusion	k_{fd} (min^{-1})	0.04123	0.02938	0.02352	0.02459
	R^2	0.9767	0.9247	0.9095	0.9680
Intraparticle diffusion	k_f (mg/g $\text{min}^{1/2}$)	0.0427	0.1783	0.5270	1.2078
	C	5.619	13.085	23.326	39.844
	R^2	0.9800	0.9447	0.9590	0.9798

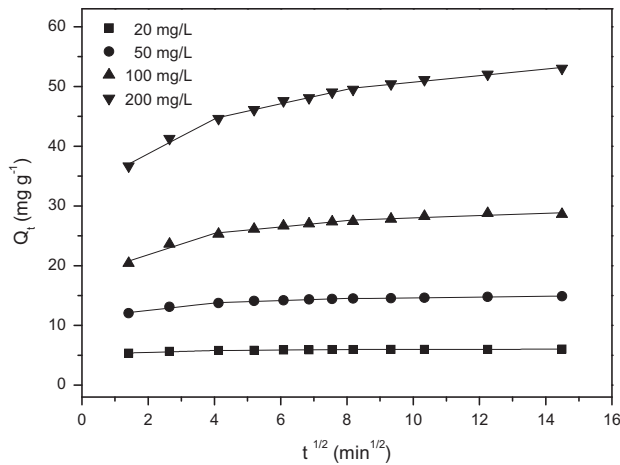


Fig. 10. The intraparticle diffusion model plots for the adsorption of RhB onto the CALP.

where C_e is the equilibrium concentration of the adsorbate (mg/L), q_e is the amount of adsorbate adsorbed per unit mass of adsorbent (mg/g), k_b is the Langmuir constant (L/mg), and q_m is the theoretical maximum adsorption capacity (mg/g).

Compared to the Langmuir isotherm, the Freundlich model is generally found to be more suitable for characterizing the multilayer adsorption process. The Freundlich adsorption isotherm can be expressed as:

$$\ln q_e = \ln k_F + \frac{\ln C_e}{n} \quad (6)$$

where n and k_F are Freundlich adsorption isotherm constants, n indicates how favorable the adsorption process is, and k_F is the adsorption capacity of the adsorbent.

Koble–Corrigan isotherm is a three-parameter model, which incorporated the Langmuir and Freundlich isotherm equations to fit the equilibrium adsorption data [28]. The Koble–Corrigan equation is represented as:

$$q_e = \frac{AC_e^m}{1 + BC_e^m} \quad (7)$$

where A , B , and m are the Koble–Corrigan isotherm constants, obtained from nonlinear regressive analysis of Koble–Corrigan isotherm.

The adsorption equilibrium data were evaluated by the aforementioned isotherm equations, and the corresponding calculated parameters are given in Table 3. The Langmuir model assumes that adsorption takes place on a homogeneous-adsorbent surface of identical sites that are equally available and energetically equivalent. However, application of the Langmuir model to the present experimental data gave a poor fit, so that it is clearly not appropriate for this system. As observed, the value of R^2 obtained from Freundlich isotherm equation was higher than that from Langmuir isotherm, which indicated that the adsorption of RhB takes place on a heterogeneous adsorbent surface. The equilibrium data were well fitted by Koble–Corrigan model with correlation coefficients $R^2 > 0.995$. The Koble–Corrigan isotherm is shown in Fig. 11. The Koble–Corrigan isotherm was an appropriate model to explain the mechanism of RhB adsorbed onto the CALP. The similar result was also observed in the adsorption of MB on the lotus leaf powder [21].

3.7. Thermodynamic studies

Thermodynamic parameters, such as free energy change ΔG° (kJ/mol), enthalpy change ΔH° (kJ/mol), and entropy change ΔS° (J/(mol K)) of adsorption were determined by the following equations:

$$K_d = \frac{C_{ad,e}}{C_e} \quad (8)$$

$$\Delta G^\circ = -RT \ln K_d \quad (9)$$

$$\ln K_d = \frac{\Delta H^\circ}{-RT} + \frac{\Delta S^\circ}{R} \quad (10)$$

Table 3
Langmuir, Freundlich, and Koble–Corrigan constants for the adsorption of RhB onto the CALP

Temperature (°C)	Langmuir			Freundlich			Koble–Corrigan			
	q_m (mg/g)	k_b (L/mg)	R^2	k_F	$1/n$	R^2	A	B	m	R^2
30	104.8	0.0487	0.977	8.161	0.598	0.980	4.892	0.0443	1.012	0.998
40	134.6	0.0309	0.914	6.641	0.672	0.958	2.116	0.0231	1.405	0.995
50	118.9	0.0294	0.804	5.690	0.679	0.954	1.415	0.0165	1.489	0.998

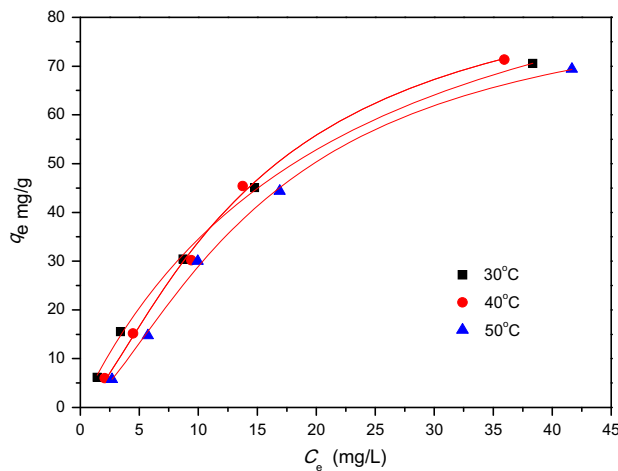


Fig. 11. Koble–Corrigan isotherms for the adsorption of RhB onto the CALP.

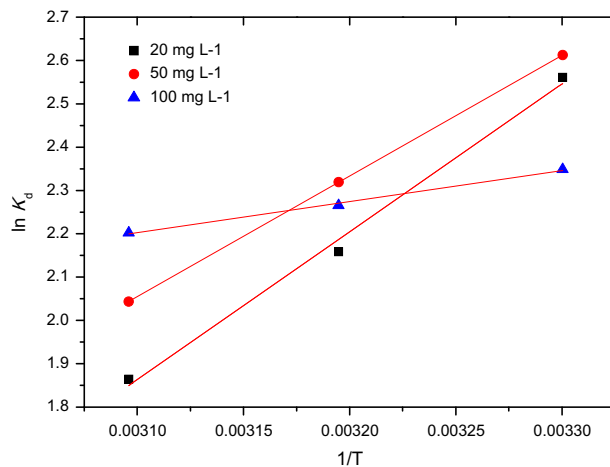


Fig. 12. Plots of $\ln K_d$ against $1/T$ for adsorption of RhB onto the CALP at different concentrations.

where K_d is the equilibrium constant, C_e is the equilibrium concentration in solution (mg/L), and $C_{ad/e}$ is the amount of RhB adsorbed on the adsorbent per liter of solution at equilibrium (mg/L), R is the gas constant (8.314 J/mol/K), T is the absolute temperature (K). The values of ΔH° and ΔS° are determined from the slope and intercept of the plots of $\ln K_d$ vs. $1/T$ (Fig. 12). The calculated values of ΔH° , ΔS° , and ΔG° are presented in Table 4. The negative ΔG° value indicates the process to be feasible and spontaneous nature of adsorption. The negative values of ΔH° supported an exothermic nature of adsorption and the ΔS° was also negative, which suggests a decrease in the freedom of the system.

4. Conclusions

In the present study, the removal of RhB from aqueous solution was investigated using natural CALP. The CALP exhibited good adsorption for RhB over a wide pH range of 2–11. The CALP had buffering action on the RhB/CALP system to maintain the solution pH in the range 7. The RhB adsorption process followed the pseudo-second-order model, suggesting that the adsorption might be a chemisorption process involving valence forces by sharing or exchanging the electrons between adsorbent and adsorbate. The Langmuir, Freundlich, and Koble–Corrigan isotherm were used to discuss the adsorption behavior and the best fits of the equilibrium data were provided by Koble–Corrigan isotherm ($R^2 > 0.99$). Thermodynamic parameters, such as free energy change ΔG° , enthalpy change ΔH° , and entropy change ΔS° of adsorption RhB dye onto the CALP were exothermic and spontaneous process. In conclusion, the CALP could be a low-cost, natural, and effective adsorbent for the removal of synthetic dye pollutants from the wastewater.

Table 4
Thermodynamic parameters for the adsorption of RhB onto the CALP

C_0 (mg/L)	ΔH° (kJ/mol)	ΔS° (J/mol/K)	ΔG° (kJ/mol)		
			30°C	40°C	50°C
20	−28.373	−72.46	−6.416	−5.692	−4.967
50	−23.153	−54.69	−6.582	−6.035	−5.488
100	−5.959	−0.16	−5.912	−5.910	−5.908

Acknowledgements

This work was supported by Ningbo Natural Science Foundation (2014A610093, 2014A610097), Ningbo Science and Technology Plan Projects (2014C50007, 2014C50008), and Zhejiang Provincial Natural Science Foundation of China under Grant No. LQ14E090003.

References

- [1] X.Z. Bu, G.K. Zhang, Y.D. Guo, Thermal modified palygorskite: Preparation, characterization, and application for cationic dye-containing wastewater purification, *Desalin. Water Treat.* 30 (2011) 339–347.
- [2] R. Jain, M. Mathur, S. Sikarwar, A. Mittal, Removal of the hazardous dye Rhodamine B through photocatalytic and adsorption treatments, *J. Environ. Manage.* 85 (2007) 956–964.
- [3] J.C. Garcia, J.L. Oliveira, A.E.C. Silva, C.C. Oliveira, J. Nozaki, N.E. Desouza, Comparative study of the degradation of real textile effluents by photocatalytic reactions involving UV/TiO₂/H₂O₂ and UV/Fe²⁺/H₂O₂ systems, *J. Hazard. Mater.* 147 (2007) 105–110.
- [4] T. Shimada, H. Yamazaki, M. Mimura, Y. Inui, F.P. Guengerich, Interindividual variations in human liver cytochrome P-450 enzymes involved in the oxidation of drugs, carcinogens, toxic chemicals: studies with liver microsomes of 30 Japanese, 30 Caucasians, *J. Pharmacol. Exp. Ther.* 270 (1994) 414–423.
- [5] D. Kornbrust, T. Barfknecht, Testing of 24 food, drug, cosmetic, and fabric dyes in the in vitro and the in vivo/in vitro rat hepatocyte primary culture DNA repair assays, *Environ. Mutagen.* 7 (1985) 101–120.
- [6] V.K. Gupta, A. Mittal, L. Kurup, J. Mittal, Adsorption of a hazardous dye, erythrosine, over hen feathers, *J. Colloid Interface Sci.* 304 (2006) 52–57.
- [7] A.E. Ofomaja, Equilibrium sorption of methylene blue using mansonia wood sawdust as biosorbent, *Desalin. Water Treat.* 3 (2009) 1944–3994.
- [8] G. Atun, G. Hisarlı, A.E. Kurtoğlu, N. Ayar, A comparison of basic dye adsorption onto zeolitic materials synthesized from fly ash, *J. Hazard. Mater.* 187 (2011) 562–573.
- [9] T.A. Khan, S. Dahiya, I. Ali, Use of kaolinite as adsorbent: Equilibrium, dynamics and thermodynamic studies on the adsorption of Rhodamine B from aqueous solution, *Appl. Clay Sci.* 69 (2012) 58–66.
- [10] B. Ismail, S.T. Hussain, S. Akram, Adsorption of methylene blue onto spinel magnesium aluminate nanoparticles: Adsorption isotherms, kinetic and thermodynamic studies, *Chem. Eng. J.* 219 (2013) 395–402.
- [11] R.M. Gong, S.X. Zhu, D.M. Zhang, J. Chen, S.J. Ni, R. Guan, Adsorption behavior of cationic dyes on citric acid esterifying wheat straw: Kinetic and thermodynamic profile, *Desalination* 230 (2008) 220–228.
- [12] E.L.K. Mui, W.H. Cheung, M. Valix, G. McKay, Dye adsorption onto char from bamboo, *J. Hazard. Mater.* 177 (2010) 1001–1005.
- [13] T.A. Khan, S. Sharma, E.A. Khan, A.A. Mukhlif, Removal of congo red and basic violet 1 by chir pine (*Pinus roxburghii*) sawdust, a saw mill waste: batch and column studies, *Toxicol. Environ. Chem.* 96 (2014) 555–568.
- [14] B.H. Hameed, M.I. El-Khaiary, Sorption kinetics and isotherm studies of a cationic dye using agricultural waste: Broad bean peels, *J. Hazard. Mater.* 154 (2008) 639–648.
- [15] N.M. Mahmoodi, B. Hayati, M. Arami, C. Lan, Adsorption of textile dyes on pine cone from colored wastewater: Kinetic, equilibrium and thermodynamic studies, *Desalination* 268 (2011) 117–125.
- [16] T.A. Khan, M. Nazir, E.A. Khan, Adsorptive removal of Rhodamine B from textile wastewater using water chestnut (*Trapa natans* L.) peel: Adsorption dynamics and kinetic studies, *Toxicol. Environ. Chem.* 95 (2013) 918–931.
- [17] P. Mohammad, R.K. Ahmad, Adsorption of methylene blue onto *Platanus orientalis* leaf powder: Kinetic, equilibrium and thermodynamic studies, *Ind. Eng. Chem.* 21 (2015) 1014–1019.
- [18] S. Liang, X.Y. Guo, N.C. Feng, Q.H. Tian, Isotherms, kinetics and thermodynamic studies of adsorption of Cu²⁺ from aqueous solutions by Mg²⁺/K⁺ type orange peel adsorbents, *J. Hazard. Mater.* 174 (2010) 756–762.
- [19] Y.S. Ho, G. McKay, Sorption of dye from aqueous solution by peat, *Chem. Eng. J.* 70 (1998) 115–124.
- [20] S.J. Allen, Q. Gan, R. Matthews, P.A. Johnson, Kinetic modeling of the adsorption of basic dyes by kudzu, *J. Colloid Interface Sci.* 286 (2005) 101–109.
- [21] X.L. Han, W. Wang, X.J. Ma, Adsorption characteristics of methylene blue onto low cost biomass material lotus leaf, *Chem. Eng. J.* 171 (2011) 1–8.
- [22] M. Uğurlu, Adsorption of a textile dye onto activated sepiolite, *Microporous Mesoporous Mater.* 119 (2009) 276–283.
- [23] V. Ponnusami, K.S. Rajan, S.N. Srivastava, Application of film-pore diffusion model for methylene blue adsorption onto plant leaf powders, *Chem. Eng. J.* 163 (2010) 236–242.
- [24] A. Olgun, N. Atar, Equilibrium and kinetic adsorption study of Basic Yellow 28 and Basic Red 46 by a boron industry waste, *J. Hazard. Mater.* 161 (2009) 148–156.
- [25] L. Abramian, H. El-Rassy, Adsorption kinetics and thermodynamics of azo-dye Orange II onto highly porous titania aerogel, *Chem. Eng. J.* 150 (2009) 403–410.
- [26] A. Khaled, A.E. Nemr, A. El-Sikaily, O. Abdelwahab, Removal of Direct N Blue-106 from artificial textile dye effluent using activated carbon from orange peel: Adsorption isotherm and kinetic studies, *J. Hazard. Mater.* 165 (2009) 100–110.
- [27] Z. Baysal, E. Çinar, Y. Bulut, H. Alkan, M. Dogru, Equilibrium and thermodynamic studies on biosorption of Pb(II) onto *Candida albicans* biomass, *J. Hazard. Mater.* 161 (2009) 62–67.
- [28] R.A. Koble, T.E. Corrigan, Adsorption isotherms for pure hydrocarbons, *Ind. Eng. Chem.* 44 (1952) 383–387.